Relativistic many-body calculations of transition rates from core-excited states in sodiumlike ions

U. I. Safronova,* W. R. Johnson,† and M. S. Safronova‡
Department of Physics, University of Notre Dame, 225 Nieuwland Science Hall, Notre Dame, Indiana 46566

J. R. Albritton
Lawrence Livermore National Laboratory, P.O. Box 808, Livermore, California 94551
(Received 13 August 2002; published 26 November 2002; publisher error corrected 29 July 2003)

Rates and line strengths are calculated for the $2s^22p^53l3l'$-$2s^22p^63l''$ and $2s2p^63l3l'$-$2s^22p^63l''$ electric-dipole ($E1$) transitions in Na-like ions with nuclear charges ranging from $Z=14$ to 100. Relativistic many-body perturbation theory (RMBPT), including the Breit interaction, is used to evaluate retarded $E1$ matrix elements in length and velocity forms. The calculations start from a $1s^22s^22p^6$ Dirac-Fock potential. First-order RMBPT is used to obtain intermediate coupling coefficients and second-order RMBPT is used to calculate transition matrix elements. A detailed discussion of the various contributions to dipole matrix elements is given for sodiumlike copper ($Z=29$). Transition energies used in the calculation of transition rates are from second-order RMBPT. Trends of transition rates as functions of Z are shown graphically for selected transitions.

DOI: 10.1103/PhysRevA.66.052511 PACS number(s): 31.15.Ar, 31.15.Md, 31.25.Jf, 32.30.Rj

I. INTRODUCTION

Transitions from $2s^22p^53l3l'$ and $2s2p^63l3l'$ states to the ground ($2s^22p^63s$) or singly excited ($2s^22p^63p$ and $2s^22p^63d$) states form satellite lines to the bright electric-dipole ($E1$) lines created by transitions from $2s^22p^53l$ and $2s2p^63l$ states to the ground state ($2s^22p^6$) in Ne-like ions. These core-excited $2s^22p^53l3l'$ and $2s2p^63l3l'$ states (often called doubly excited states) in sodiumlike ions have been studied extensively both experimentally and theoretically over the past 20–30 years.

Transition rates and oscillator strengths for Na-like ions have been calculated using multiconfiguration Dirac-Fock (MCDF) [1,2] and multiconfiguration Hartree-Fock (MCHF) [3–5] methods. Recently, *R*-matrix calculations of electron-impact collision strengths for excitations from the inner L shell into doubly excited states of Fe^{15+} were presented by Bautista [6]. Energies of $2s^22p^63l$ and $2s^22p^53l3l'$ states were calculated in that paper using the SUPERSTRUCTURE code [7]. It was shown in [6] that the disagreement between the calculated data and the data recommended by Sugar and Corliss [8] and Shirai *et al.* [9] ranges from 0.5% to 5%.

Experimentally, the core-excited $2s^22p^53l3l'$ and $2s2p^63l3l'$ states were studied by the beam-foil technique [10,11], photoemission [12–21], and Auger spectroscopy [22–26]. Strong line radiation involving $n=3$ to $n=2$ transitions in Ne-like ions together with satellite lines of Na-like ions have been observed from laser-produced plasmas [12–16], X pinch, [17], tokamaks [18,19], electron beam ion trap (EBIT) [20], and solar flares [21]. The identification of measured spectral lines was based on theoretical calculations carried out primarily using the MCDF method with Cowan's code [27].

In this paper, we present a comprehensive set of calculations for $2s^22p^53l3l'$-$2s^22p^63l''$ and $2s2p^63l3l'$-$2s^22p^63l''$ transitions to compare with previous calculations and experiments. Our aim is to provide benchmark values for the entire Na isoelectronic sequence. The large number of possible transitions has made experimental identification difficult. Experimental verifications should become simpler and more reliable using this more accurate set of calculations.

Relativistic many-body perturbation theory (RMBPT) is used here to determine matrix elements and transition rates for allowed and forbidden electric-dipole transitions between the odd-parity core-excited states ($2s^22p^53s^2+2s^22p^53p^2+2s^22p^53d^2+2s^22p^53s3d+2s2p^63s3p+2s2p^63p3d$) and the ground state ($2s^22p^63s$) together with the two singly excited states ($2s^22p^63d$) and between the even-parity core-excited states ($2s^22p^53s3p+2s^22p^53p3d+2s2p^63s^2+2s2p^63p^2+2s2p^63d^2+2s2p^63s3d$) and the two singly excited states ($2s^22p^63p$) in Na-like ions with nuclear charges ranging from $Z=14$ to 100. Retarded $E1$ matrix elements are evaluated in both length and velocity forms. These calculations start from a Ne-like core Dirac-Fock (DF) potential. First-order perturbation theory is used to obtain intermediate coupling coefficients and second-order RMBPT is used to determine transition matrix elements. The energies used in the calculation of transition rates are obtained from second-order RMBPT.

II. METHOD

In this section, we discuss relativistic RMBPT for first- and second-order transition matrix elements for atomic systems with two valence electrons and one hole. Details of the RMBPT method for calculation of radiative transition rates for systems with one valence electron and one hole were presented for Ne-like and Ni-like ions in [28,29]. Here, we follow the pattern of the corresponding calculation in Refs. [28,29] but limit our discussion to the model space and the

*Electronic address: usafrono@nd.edu
†Electronic address: johnson@nd.edu; URL: www.nd.edu/~johnson
‡Present address: Electron and Optical Physics Division, National Institute of Standards and Technology, Gaithersburg, MD 20899-8410.

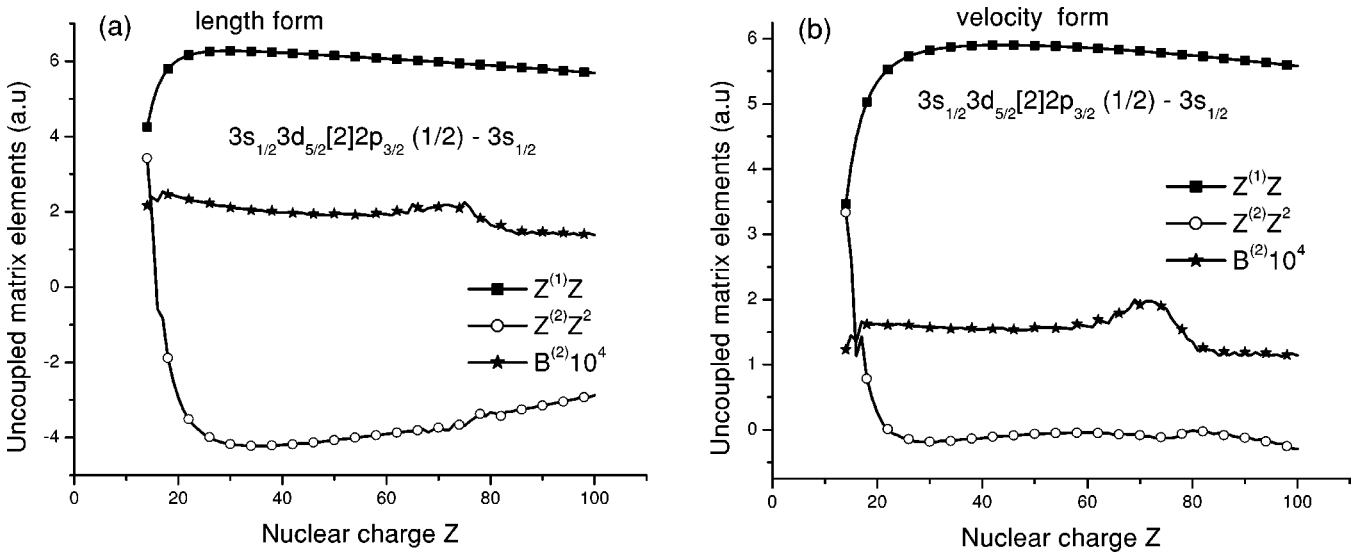

FIG. 1. Uncoupled matrix element for the $3s3d_{5/2}[2]2p_{3/2}(1/2)$-$3s$ transition calculated in length and velocity forms in Na-like ions.

first- and second-order particle-particle-hole diagram contributions in Na-like ions.

A. Model space

For Na-like ions with two electrons above the Ne-like $(1s^2 2s^2 2p_{1/2}^2 2p_{3/2}^4)$ core and one hole in the core, the model space is formed from particle-particle-hole states of the type $a_v^\dagger a_w^\dagger a_a|0\rangle$, where $|0\rangle$ is the core state function. The indices v and w designate valence electrons and a designates a core electron. For our study of low-lying $3l3l'2l^{-1}$ states of Na-like ions, the index a ranges over $2s$, $2p_{1/2}$, and $2p_{3/2}$, while v and w range over $3s$, $3p_{1/2}$, $3p_{3/2}$, $3d_{3/2}$, and $3d_{5/2}$. To obtain orthonormal model states, we consider the coupled states (vwa) defined by

$$\Psi(QJM)=N(Q)\sum \langle vw|K_{12}\rangle\langle K_{12}a|K\rangle a_v^\dagger a_w^\dagger a_a|0\rangle, \quad (1)$$

where Q describes a particle-particle-hole state with quantum numbers $n_v\kappa_v n_w\kappa_w[J_{12}]n_a\kappa_a$ and intermediate momentum J_{12}. We use the notation $K_i=\{J_i,M_i\}$ and $v=\{j_v,m_v\}$. The sum in Eq. (1) is over magnetic quantum numbers m_v,m_w,m_a, and M_{12}. The quantity $\langle K_1K_2|K_3\rangle$ is a Clebsch-Gordan coefficient:

$$\langle K_1K_2|K_3\rangle=(-1)^{J_1-J_2+M_3}\sqrt{[J_3]}\begin{pmatrix} J_1 & J_2 & J_3 \\ M_1 & M_2 & -M_3 \end{pmatrix}, \quad (2)$$

where $[J]=2J+1$. Combining two $n=3$ particles with possible intermediate momenta and $n=2$ hole orbitals in sodium, we obtain 121 odd-parity states with $J=1/2,\ldots,11/2$ and 116 even-parity states with $J=1/2,\ldots,11/2$. The distribution of the 237 states in the model space is found in Table I of the accompanying EPAPS document [30]. Instead of using the $3l'3l''[J_1]2l^{-1}(J)$ designations, we use the simpler designations $3l'3l''[J_1]2l(J)$ in the tables and text below.

B. Dipole matrix element

The first- and second-order reduced $E1$ matrix elements $Z^{(1)}$ and $Z^{(2)}$ and the second-order Breit correction to the reduced $E1$ matrix element $B^{(2)}$ for a transition between the uncoupled particle-particle-hole state $\Psi(QJM)$ of Eq. (1) and the one-particle state $a_x^\dagger|0\rangle$ are given in Appendix.

The uncoupled reduced matrix elements are calculated in both length and velocity gauges. Differences between length and velocity forms are illustrated for the uncoupled $[3s3d_{5/2}[2]2p_{3/2}(1/2)$-$3s]$ matrix element in panels (a) and (b) of Fig. 1. In the high-Z limit, $Z^{(1)}$ is proportional to $1/Z$, $Z^{(2)}$ is proportional to $1/Z^2$, and $B^{(2)}$ is independent of Z (see [31]). Taking into account this Z dependence, we plot $Z^{(1)}\times Z, Z^{(2)}\times Z^2$, and $B^{(2)}\times 10^4$ in the figure. The contribution of the second-order matrix elements $Z^{(2)}$ is seen to be much larger in length form. The differences between results in length and velocity forms shown in Fig. 1 are precisely compensated by "derivative terms" $P^{(\mathrm{derv})}$, as shown later.

C. Dipole matrix elements in Cu^{18+}

In Table I, we list values of *uncoupled* first- and second-order dipole matrix elements $Z^{(1)}$, $Z^{(2)}$, $B^{(2)}$, together with derivative terms $P^{(\mathrm{derv})}$ for Na-like copper, $Z=29$. For simplicity, we only list values for selected dipole transitions between odd-parity states with $J=1/2$ and the ground $3s$ and excited $3d_{3/2}$ states. Uncoupled matrix elements for other transitions in Na-like copper are given in Table II of the accompanying EPAPS document [30]. The derivative terms shown in Table I arise because transition amplitudes depend on energy, and the transition energy changes order by order in RMBPT calculations. Both length (L) and velocity (V) forms are given for the matrix elements. We find that the first-order matrix elements $Z_L^{(1)}$ and $Z_V^{(1)}$ differ by 10%; the L-V differences between second-order matrix elements are much larger for some transitions. The term $P^{(\mathrm{derv})}$ in length form almost equals $Z^{(1)}$ in length form but $P^{(\mathrm{derv})}$ in velocity form is smaller than $Z^{(1)}$ in velocity form by three to four orders of magnitude.

TABLE I. Uncoupled reduced matrix elements in length L and velocity V forms for transitions between the selected odd-parity core-excited states with $J=1/2$ and the ground $3s$ and singly excited $3d_{3/2}$ states in Cu^{18+} ion.

$3lj3l'j'(J_1)2l''j''$	$Z_L^{(1)}$	$Z_V^{(1)}$	$Z_L^{(2)}$	$Z_V^{(2)}$	$B_L^{(2)}$	$B_V^{(2)}$	$P_L^{(\mathrm{derv})}$	$P_V^{(\mathrm{derv})}$
				$[3lj3l'j'[J_1]2l''j''(1/2)\text{-}3s_{1/2}]$ transitions				
$3s_{1/2}3s_{1/2}[0]2p_{1/2}$	−0.040775	−0.037586	−0.003606	−0.002838	−0.000116	−0.000104	−0.040564	0.000139
$3s_{1/2}3d_{3/2}[1]2p_{3/2}$	−0.057161	−0.052902	0.001364	0.000191	−0.000070	−0.000108	−0.057130	−0.000115
$3p_{1/2}3p_{3/2}[1]2p_{3/2}$	0.000000	0.000000	−0.000160	−0.000141	−0.000002	−0.000003	0.000000	0.000000
$3p_{1/2}3p_{3/2}[2]2p_{3/2}$	0.000000	0.000000	−0.001048	−0.001313	0.000002	0.000003	0.000000	0.000000
$3p_{3/2}3p_{3/2}[2]2p_{3/2}$	0.000000	0.000000	−0.000889	−0.001067	−0.000002	−0.000001	0.000000	0.000000
				$[3lj3l'j'[J_1]2l''j''(1/2)\text{-}3d_{3/2}]$ transitions				
$3s_{1/2}3s_{1/2}[0]2p_{1/2}$	0.000000	0.000000	0.000388	−0.000293	0.000006	0.000003	0.000000	0.000000
$3s_{1/2}3d_{3/2}[1]2p_{3/2}$	0.012526	0.011536	0.001077	0.000835	0.000027	0.000013	0.012483	−0.000003
$3p_{1/2}3p_{3/2}[1]2p_{3/2}$	0.000000	0.000000	0.000205	0.000602	−0.000001	−0.000001	0.000000	0.000000
$3p_{1/2}3p_{3/2}[2]2p_{3/2}$	0.000000	0.000000	0.000720	−0.000132	−0.000002	0.000001	0.000000	0.000000
$3p_{3/2}3p_{3/2}[2]2p_{3/2}$	0.000000	0.000000	0.000671	0.000436	0.000004	0.000002	0.000000	0.000000

Although we use an intermediate-coupling scheme, it is nevertheless convenient to label the physical states using the LS scheme. The length and velocity forms of coupled matrix elements differ only in the fourth or fifth digits. These L-V differences arise because we start our RMBPT calculations using a nonlocal Dirac-Fock potential. If we were to replace the DF potential by a local potential, the differences would disappear completely. Removing the second-order contribution increases L-V differences by a factor of 10. Values of *coupled* reduced matrix elements in length and velocity forms are given in Table III of the accompanying EPAPS document [30]. Theoretical wavelengths λ and transition probabilities A_r for selected transitions in Na-like from $Z=26$ up to $Z=30$ are given in Table IV of [30].

III. RESULTS AND COMPARISON WITH OTHER THEORY AND EXPERIMENT

Trends of the Z dependence of transition rates for the transitions from core-excited even-parity states with $J=1/2$ to two possible singly excited odd-parity states are presented in Fig. 2. Figures for transitions from other states are found in the accompanying EPAPS document [30].

We find that transitions with smooth Z dependence are rarer than transitions with sharp features. Smooth Z dependence occurs for transitions from doublet and quartet core-excited states. Usually, singularities occur in the intermediate interval of $Z=25$–50 when neither the LS nor the jj coupling scheme describes the states of these ions properly. One general conclusion that can be derived from the figures is that the smooth Z dependence occurs more frequently for transitions from low-lying core-excited states.

Singularities in the transition rate curves have two distinct origins: avoided level crossings and zeros in dipole matrix elements. Avoided level crossings result in changes of the dominant configuration of a state at a particular value of Z and lead to abrupt changes in the transition rate curves when the partial rates associated with the dominant configurations below and above the crossing point are significantly different. Zeros in transition matrix elements lead to cusplike minima in the transition rate curves. Examples of each of these two singularity types can be seen in Fig. 2.

In Table II, we present data for transitions from odd-parity states with $J=1/2$ in Fe^{15+} and Xe^{43+}. We compare the present RMBPT values with those given by Nilsen [2]. More complete comparisons are given in the accompanying EPAPS document [30]. The calculations of [2] were based on a multiconfigurational relativistic bound-state and distorted-wave continuum code (YODA). Since jj labeling was used in [2], we keep that labeling in Table II. We find that the A_r values from RMBPT and YODA differ by 10% in most cases. The differences are explained by the second-order corrections to dipole matrix elements included in RMBPT.

In Tables III–V, wavelengths and electric-dipole transition rates are presented for transitions in Na-like Fe, Co, Ni, Cu, and Zn. We limit the tables to the transitions given in Refs. [12,14,20]. Measurements for Fe^{15+} are presented in Tables III and IV since two different ranges of spectra were investigated in Ref. [12] (16.8–17.8 Å) and Ref. [14] (15.1–15.5 Å). Three lines for Fe^{15+} were identified in the region 15.1–15.26 Å by Brown *et al.* in Ref. [20]. All possible $3l_1j_1 3l_2j_2[J_1]2l_3j_3(J)\text{-}3l_j$ transitions produce 393 spectrum lines. These lines in Fe^{15+} are covered by four spectral regions; 12.5–14.2 Å (114 lines), 15.1–15.9 Å (174 lines), 16.8–17.9 Å (102 lines), and 19.3–19.7 Å (three lines). The first 114 lines are from $3dj_1 3dj_2[J_1]2s(J)-3l_j$ and $3pj_1 3dj_2[J_1]2s_{1/2}(J)-3l_j$ transitions and the last three lines are from $3s3s[0]2p_j(J)-3d_j$ transitions. Our RMBPT data together with experimental measurements for Fe^{15+} in the region of 16.8–17.8 Å and 15.1–15.5 Å are presented in Tables III and IV, respectively. The agreement between our RMBPT wavelengths and the experimental values is within 0.02–0.04% for both regions of the spectrum.

IV. CONCLUSION

We have presented a systematic second-order relativistic MBPT study of reduced matrix elements and transition rates

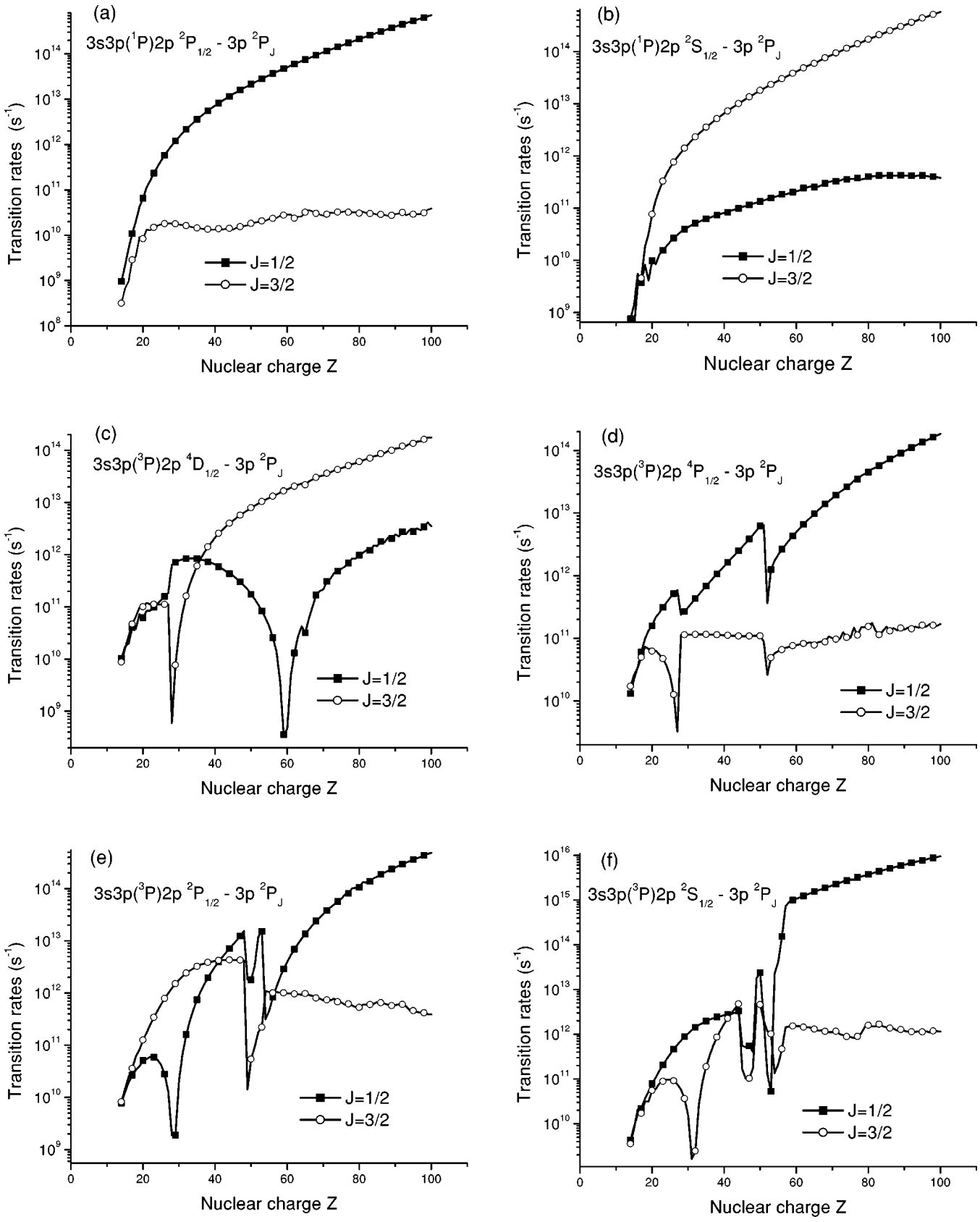

FIG. 2. Transition rates for the transitions from core-excited even-parity states with $J=1/2$ as a function of Z in Na-like ions.

TABLE II. Wavelengths (λ in angstroms) and transition rates (A_r in s^{-1}) for transitions from core-excited states $QJ(Q=3lj3l'j'[J_1]2l''j'', J=1/2)$ to the ground state in Na-like ions. Comparison with theoretical data was obtained by using the YODA code from Ref. [2]. Numbers in brackets represent powers of 10.

Q	$Z=26$				$Z=54$			
	λ_{RMBPT}	λ_{YODA}	A_r^{RMBPT}	A_r^{YODA}	λ_{RMBPT}	λ_{YODA}	A_r^{RMBPT}	A_r^{YODA}
$3s_{1/2}3s_{1/2}[0]2p_{1/2}$	17.0747	17.1207	8.096[11]	8.27[11]	2.7865	2.7884	2.507[12]	2.62[12]
$3s_{1/2}3d_{3/2}[1]2p_{3/2}$	15.9418	15.9883	9.449[10]	1.10[11]	2.7731	2.7747	9.345[10]	6.70[10]
$3p_{1/2}3p_{1/2}[0]2p_{1/2}$	15.6327	15.6671	2.578[09]	2.67[09]	2.7355	2.7366	2.625[14]	2.50[14]
$3s_{1/2}3d_{3/2}[2]2p_{3/2}$	15.5711	15.5958	4.600[11]	5.21[11]	2.7241	2.7251	1.724[14]	2.07[14]
$3s_{1/2}3d_{5/2}[2]2p_{3/2}$	15.5029	15.5193	3.776[12]	4.02[12]	2.6271	2.6276	4.846[11]	6.35[11]
$3p_{1/2}3p_{3/2}[1]2p_{1/2}$	15.3681	15.3884	1.465[11]	1.56[11]	2.5927	2.5939	8.932[10]	1.06[12]
$3p_{3/2}3p_{3/2}[0]2p_{1/2}$	15.3672	15.3558	9.425[08]	7.81[09]	2.5925	2.5938	9.882[11]	6.29[10]
$3s_{1/2}3d_{3/2}[1]2p_{1/2}$	15.2148	15.2174	2.240[13]	2.65[13]	2.5734	2.5748	9.387[11]	6.72[11]
$3s_{1/2}3p_{1/2}[0]2s_{1/2}$	14.0969	14.1212	2.826[10]	2.80[10]	2.5572	2.5580	5.078[13]	6.02[13]
$3d_{5/2}3d_{5/2}[0]2p_{1/2}$	13.6959	13.6884	9.156[07]	1.67[09]	2.3876	2.3881	2.952[08]	1.43[10]

TABLE III. Wavelengths (λ in angstroms) and transition rates (A_r in s^{-1}) for transitions between core-excited states $3l3l'(L_1S_1)2p\ LSJ$ and singly excited states $3l\ L'S'J'$ in Na-like ions. Comparison with experimental data (λ_{expt}) from Ref. [12]. Numbers in brackets represent powers of 10.

Upper level	Low level	$Z=26$		
		λ_{RMBPT}	λ_{expt}	A_r
$3s3p(^3P)2p\ ^2S_{1/2}$	$3p\ ^2P_{3/2}$	16.813	16.821	9.189[10]
$3s3d(^3D)2p\ ^2P_{3/2}$	$3d\ ^2D_{3/2}$	16.839	18.834	2.942[11]
$3s3p(^3P)2p\ ^2D_{3/2}$	$3p\ ^2P_{1/2}$	16.883	16.899	9.942[10]
$3s3p(^3P)2p\ ^2P_{1/2}$	$3p\ ^2P_{1/2}$	16.939	16.937	2.782[10]
$3s3d(^3D)2p\ ^2P_{1/2}$	$3d\ ^2D_{3/2}$	16.958	16.952	4.962[11]
$3s3p(^3P)2p\ ^2P_{1/2}$	$3p\ ^2P_{3/2}$	16.999	16.993	7.880[11]
$3s3d(^1D)2p\ ^2P_{3/2}$	$3d\ ^2D_{5/2}$	17.037	17.029	5.370[11]
$3p3p(^3P)2p\ ^2P_{3/2}$	$3d\ ^2D_{3/2}$	17.098	17.094	3.901[11]
$3s3d(^1D)2p\ ^2D_{5/2}$	$3d\ ^2D_{3/2}$	17.131	17.129	4.887[11]
$3s3d(^3D)2p\ ^4F_{3/2}$	$3d\ ^2D_{3/2}$	17.168	17.166	4.273[11]
$3s3p(^1P)2p\ ^2P_{3/2}$	$3p\ ^2P_{3/2}$	17.199	17.208	5.081[11]
$3s3p(^3P)2p\ ^4P_{3/2}$	$3p\ ^2P_{3/2}$	17.242	17.244	1.972[11]
$3s3p(^3P)2p\ ^4D_{1/2}$	$3p\ ^2P_{3/2}$	17.307	17.297	1.118[11]
$3s3d(^3D)2p\ ^2P_{3/2}$	$3d\ ^2D_{5/2}$	17.353	17.344	7.288[11]
$3s3s(^1S)2p\ ^2P_{3/2}$	$3s\ ^2S_{1/2}$	17.374	17.368	7.925[11]
$3p3p(^3P)2p\ ^2D_{5/2}$	$3d\ ^2D_{3/2}$	17.394	17.398	3.118[11]
$3s3d(^1D)2p\ ^2P_{1/2}$	$3d\ ^2D_{3/2}$	17.401	17.407	6.364[11]
$3s3p(^1P)2p\ ^2S_{1/2}$	$3p\ ^2P_{3/2}$	17.454	17.451	7.665[11]
$3s3p(^1P)2p\ ^2P_{1/2}$	$3p\ ^2P_{1/2}$	17.484	17.471	5.848[11]
$3s3d(^3D)2p\ ^4F_{7/2}$	$3d\ ^2D_{5/2}$	17.493	17.499	1.394[11]
$3s3p(^1P)2p\ ^2P_{1/2}$	$3p\ ^2P_{3/2}$	17.548	17.542	1.810[10]
$3p3p(^3P)2p\ ^4D_{1/2}$	$3d\ ^2D_{3/2}$	17.596	17.596	6.959[10]
$3s3p(^3P)2p\ ^4S_{3/2}$	$3p\ ^2P_{1/2}$	17.611	17.623	2.480[09]
$3s3p(^3P)2p\ ^4S_{3/2}$	$3p\ ^2P_{3/2}$	17.677	17.660	1.185[10]
$3p3p(^3P)2p\ ^4D_{5/2}$	$3d\ ^2D_{3/2}$	17.736	17.734	1.366[10]
$3p3p(^1D)2p\ ^2D_{5/2}$	$3d\ ^2D_{5/2}$	17.763	17.787	1.443[10]
$3p3p(^3P)2p\ ^4P_{3/2}$	$3d\ ^2D_{5/2}$	17.821	17.821	2.537[10]
$3p3p(^3P)2p\ ^4P_{3/2}$	$3d\ ^2D_{5/2}$	17.882	17.901	1.892[10]

for $[3l_1j_13l_2j_2[J_1]2l_3j_3(J)\text{-}3lj]$ electric-dipole transitions in sodiumlike ions with the nuclear charges Z ranging from 14 to 100. Our retarded $E1$ matrix elements include correlation corrections from Coulomb and Breit interactions. Both length and velocity forms of the matrix elements were evaluated and small differences (0.4%–1%), caused by the nonlocality of the starting DF potential, were found between the two forms. Second-order RMBPT transition energies were used in our evaluation of transition rates. These calculations were compared with other calculations and with available experimental data. For $Z \geqslant 20$, we believe that the present theoretical data are more accurate than other theoretical or experimental data for transitions between the $3l_1j_13l_2j_2[J_1]2l_3j_3(J)$ core-excited states and the $3lj$ singly excited states in Na-like ions. We hope that these results will be useful in analyzing older experiments and planning new ones. Additionally, these calculations provide basic theoretical input amplitudes for calculations of reduced matrix elements, oscillator strengths, and transition rates for Cu-like satellites to transitions in Ni-like ions.

ACKNOWLEDGMENTS

The work of W.R.J. and M.S.S. was supported in part by National Science Foundation Grant No. PHY-0139928. U.I.S. acknowledges partial support by Grant No. B516165 from Lawrence Livermore National Laboratory. The work of J.R.A. was performed under the auspices of the U.S. Department of Energy by the University of California, Lawrence Livermore National Laboratory, under Contract No. W-7405-Eng-48.

APPENDIX: THE PARTICLE-PARTICLE-HOLE DIAGRAM CONTRIBUTION FOR THE DIPOLE MATRIX ELEMENT

The first-order reduced $E1$ matrix element $Z^{(1)}$ for a transition between the uncoupled particle-particle-hole state $\Psi(QJM)$ of Eq. (1) and the one-particle state $a_x^\dagger|0\rangle$ is

TABLE IV. Wavelengths (λ in angstroms) and transition rates (A_r in s^{-1}) for transitions between core-excited states $3l3l'(L_1S_1)2p\,LSJ$ and singly excited states $3l\,L'S'J'$ in Na-like ions. Comparison with experimental data (λ_{expt}) from Ref. [14] (a) and Ref. [20] (b). Numbers in brackets represent powers of 10.

Upper level	Low level	$Z=26$			$Z=27$		
		λ_{RMBPT}	λ_{expt}	A_r	λ_{RMBPT}	λ_{expt}	A_r
$3p3d(^1S)2p\ ^2D_{3/2}$	$3p\ ^2P_{1/2}$	15.057		5.532[11]	13.667	13.667[a]	7.187[11]
$3p3d(^1S)2p\ ^2D_{5/2}$	$3p\ ^2P_{3/2}$	15.090		1.272[12]	13.704	13.707[a]	2.067[12]
$3d3d(^1S)2p\ ^2P_{1/2}$	$3d\ ^2D_{3/2}$	15.092	15.093[a]	5.375[12]	13.695		6.534[12]
$3s3d(^3D)2p\ ^2P_{3/2}$	$3s\ ^2S_{1/2}$	15.119	15.115[b]	8.210[12]	13.718		1.008[13]
$3p3d(^3D)2p\ ^2S_{1/2}$	$3p\ ^2P_{1/2}$	15.150	15.142[a]	8.704[10]	13.744		1.996[11]
$3p3d(^1S)2p\ ^2D_{3/2}$	$3p\ ^2P_{3/2}$	15.166		3.835[12]	13.775	13.773[a]	4.836[12]
$3d3d(^3P)2p\ ^2P_{3/2}$	$3d\ ^2D_{3/2}$	15.181	15.182[a]	9.080[12]	13.774		1.146[13]
$3s3d(^3D)2p\ ^2P_{1/2}$	$3s\ ^2S_{1/2}$	15.215	15.208[b]	2.240[13]	13.805		2.723[13]
$3p3d(^3P)2p\ ^2P_{1/2}$	$3p\ ^2P_{1/2}$	15.237		1.430[13]	13.823	13.823[a]	1.699[13]
$3s3d(^1D)2p\ ^2P_{3/2}$	$3s\ ^2S_{1/2}$	15.272	15.26[b]	1.340[13]	13.855		1.614[13]
$3s3d(^1D)2p\ ^2P_{3/2}$	$3s\ ^2S_{1/2}$	15.272	15.280[a]	1.340[13]	13.855		1.614[13]
$3p3d(^3P)2p\ ^2P_{1/2}$	$3p\ ^2P_{3/2}$	15.286	15.289[a]	1.536[11]	13.872		9.115[10]
$3d3d(^3F)2p\ ^2F_{5/2}$	$3d\ ^2D_{5/2}$	15.361	15.360[a]	1.002[12]	13.930		1.691[12]
$3d3d(^3F)2p\ ^2D_{5/2}$	$3d\ ^2D_{3/2}$	15.369		6.618[12]	13.943	13.940[a]	9.585[12]
$3p3d(^3D)2p\ ^4F_{3/2}$	$3p\ ^2P_{3/2}$	15.429		3.019[09]	14.014	14.015[a]	1.919[09]
$3s3d(^3D)2p\ ^4D_{3/2}$	$3s\ ^2S_{1/2}$	15.435		1.742[12]	14.004	14.000[a]	2.880[12]
$3p3d(^1D)2p\ ^2D_{3/2}$	$3p\ ^2P_{1/2}$	15.510		3.134[11]	14.079	14.078[a]	4.868[11]
$3s3d(^3D)2p\ ^2P_{3/2}$	$3s\ ^2S_{1/2}$	15.525		2.997[12]	14.091	14.093[a]	3.817[12]
$3d3d(^3F)2p\ ^4F_{3/2}$	$3d\ ^2D_{5/2}$	15.561	15.568[a]	1.746[11]	14.129		2.141[11]
$3d3d(^1D)2p\ ^2F_{7/2}$	$3d\ ^2D_{5/2}$	15.573		6.467[11]	14.143	14.148[a]	7.639[11]

TABLE V. Wavelengths (λ in angstroms) and transition rates (A_r in s^{-1}) for transitions between core-excited states $3l3l'(L_1S_1)2p\ LSJ$ and singly excited states $3l\,L'S'J'$ in Na-like ions. Comparison with experimental data (λ_{expt}) from Ref. [14]. Numbers in brackets represent powers of 10.

Upper level	Low level	$Z=29$			$Z=28$			$Z=30$		
		λ_{RMBPT}	λ_{expt}	A_r	λ_{RMBPT}	λ_{expt}	A_r	λ_{RMBPT}	λ_{expt}	A_r
$3s3s(^1S)2s\ ^2S_{1/2}$	$3p\ ^2P_{1/2}$	11.407	11.403	8.906[12]	12.466	12.461	7.918[12]	10.475	10.481	9.805[12]
$3d3d(^1S)2p\ ^2P_{1/2}$	$3d\ ^2D_{3/2}$	11.425	11.427	9.183[12]	12.484	12.492	7.808[12]	10.494	10.493	1.065[13]
$3d3d(^3P)2p\ ^2P_{3/2}$	$3d\ ^2D_{3/2}$	11.488	11.480	1.611[13]	12.554	12.556	1.383[13]	10.551		1.819[13]
$3p3d(^3D)2p\ ^2S_{1/2}$	$3p\ ^2P_{3/2}$	11.506	11.503	3.173[13]	12.572		2.698[13]	10.569		3.654[13]
$3d3d(^3F)2p\ ^2D_{3/2}$	$3d\ ^2D_{5/2}$	11.514		1.413[13]	12.581		1.236[13]	10.576	10.573	1.566[13]
$3d3d(^1G)2p\ ^2F_{7/2}$	$3d\ ^2D_{5/2}$	11.537	11.538	2.019[13]	12.592	12.596	1.686[13]	10.593		2.410[13]
$3p3d(^3P)2p\ ^2D_{3/2}$	$3p\ ^2P_{1/2}$	11.552		2.305[13]	12.624	12.623	2.555[13]	10.606		9.851[12]
$3p3d(^3P)2p\ ^4D_{3/2}$	$3p\ ^2P_{1/2}$	11.560	11.561	1.012[13]	12.639		3.548[12]	10.616		2.617[13]
$3d3d(^3F)2p\ ^2F_{5/2}$	$3d\ ^2D_{5/2}$	11.615		3.112[12]	12.694		2.364[12]	10.664	10.664	4.022[12]
$3p3d(^3P)2p\ ^2P_{3/2}$	$3p\ ^2P_{3/2}$	11.624	11.620	1.252[12]	12.706	12.700	9.215[11]	10.674		1.493[12]
$3d3d(^3F)2p\ ^2D_{5/2}$	$3d\ ^2D_{5/2}$	11.634		1.438[12]	12.714		1.553[12]	10.683	10.687	1.858[12]
$3d3d(^3P)2p\ ^4S_{3/2}$	$3d\ ^2D_{5/2}$	11.662		4.945[12]	12.730	12.736	3.862[12]	10.723	10.721	6.355[12]
$3p3d(^3D)2p\ ^4D_{5/2}$	$3p\ ^2P_{3/2}$	11.673	11.673	9.418[11]	12.744		1.890[09]	10.729		2.888[12]
$3s3d(^3D)2p\ ^4D_{3/2}$	$3s\ ^2S_{1/2}$	11.688	11.685	7.023[12]	12.767		4.600[12]	10.740	10.738	1.021[13]
$3d3d(^3P)2p\ ^4D_{1/2}$	$3d\ ^2D_{3/2}$	11.701		1.809[13]	12.775	12.772	1.361[13]	10.758		2.344[13]
$3d3d(^3F)2p\ ^4F_{5/2}$	$3d\ ^2D_{3/2}$	11.723		9.844[12]	12.804		6.190[12]	10.774	10.778	1.268[13]
$3s3d(^3D)2p\ ^4D_{1/2}$	$3s\ ^2S_{1/2}$	11.736	11.737	7.629[12]	12.822		6.064[12]	10.782		9.682[12]
$3d3d(^1G)2p\ ^2G_{7/2}$	$3d\ ^2D_{5/2}$	11.755	11.755	7.229[12]	12.836	12.835	5.328[12]	10.825		9.462[12]
$3p3d(^3D)2p\ ^4D_{1/2}$	$3p\ ^2P_{3/2}$	11.785	11.784	5.716[11]	12.864		4.781[11]	10.837		6.885[11]

$$Z^{(1)}(v^0w^0[J_{12}]aJ,xJ') = \sum_{vw} \sqrt{[J_{12}][J]}P_{J_{12}}(v^0v,w^0w)\,\delta(J'x) \times \delta(vx)Z(va)\begin{Bmatrix} j_x & J & 1 \\ j_a & j_w & J_{12} \end{Bmatrix}(-1)^{-j_a+j_w}, \tag{A1}$$

where v,w range over $\{v^0,w^0\}$. The quantity $P_J(v^0v,w^0w)$ is a symmetry coefficient defined by

$$P_J(v^0v,w^0w) = \eta_{v^0w^0}[\,\delta_{v^0v}\delta_{w^0w} + (-1)^{j_v+j_w+J+1}\delta_{v^0w}\delta_{w^0v}], \tag{A2}$$

where η_{vw} is a normalization factor given by

$$\eta_{vw} = \begin{cases} 1 & \text{for } w \neq v, \\ 1/\sqrt{2} & \text{for } w = v. \end{cases}$$

The dipole matrix element $Z(va)$, which includes retardation, is given in velocity and length forms in Eqs. (3) and (4) of Ref. [31]. The second-order reduced matrix element $Z^{(2)}(v^0w^0[J_{12}]aJ,xJ')$ consists of four contributions: $Z^{(\mathrm{HF})}$, $Z^{(\mathrm{RPA})}$, $Z^{(\mathrm{corr})}$, and $Z^{(\mathrm{derv})}$:

$$Z^{(\mathrm{HF})}(v^0w^0[J_{12}]aJ,xJ') = \sum_{vw} \sqrt{[J_{12}][J]}P_{J_{12}}(v^0v,w^0w)\,\delta(J'x)\,\delta(vx) \times (-1)^{-j_a+j_w}\begin{Bmatrix} j_x & J & 1 \\ j_a & j_w & J_{12} \end{Bmatrix}\sum_i \left[\frac{\delta(j_wj_i)\Delta(wi)Z(ia)}{\epsilon(w)-\epsilon(i)} + \frac{\Delta(ia)\delta(j_a,j_i)Z(wi)}{\epsilon(a)-\epsilon(i)}\right],$$

$$Z^{(\mathrm{RPA})}(v^0w^0[J_{12}]aJ,xJ') = \frac{1}{3}\sum_{vw} \sqrt{[J_{12}][J]}P_{J_{12}}(v^0v,w^0w)\,\delta(J'x)\,\delta(vx)\begin{Bmatrix} j_x & J & 1 \\ j_a & j_w & J_{12} \end{Bmatrix} \times (-1)^{-j_a+j_w}\sum_{nb}\left[\frac{Z_1(wban)Z(bn)}{\epsilon(b)+\epsilon(w)-\epsilon(a)-\epsilon(n)} + \frac{Z_1(wnab)Z(nb)}{\epsilon(b)+\epsilon(a)-\epsilon(w)-\epsilon(n)}\right], \tag{A3}$$

$$\begin{aligned} Z^{(\mathrm{corr})}(v^0w^0[J_{12}]aJ,xJ') = {} & \sum_{vw} \sqrt{[J_{12}][J]}P_{J_{12}}(v^0v,w^0w)\,\delta(J'x) \\ & \times \sum_k (-1)^{j_a-j_v+J_{12}+k}\sum_i \left[\frac{Z(ix)X_k(vwai)}{\epsilon(v)+\epsilon(w)-\epsilon(a)-\epsilon(i)}\,\delta(J,j_i)\frac{1}{[J]}\begin{Bmatrix} j_w & j_i & k \\ j_a & j_v & J_{12} \end{Bmatrix}\right. \\ & - \frac{Z(ia)X_k(vwxi)}{\epsilon(v)+\epsilon(w)-\epsilon(x)-\epsilon(i)}\begin{Bmatrix} j_x & j_i & J_{12} \\ j_w & j_v & k \end{Bmatrix}\begin{Bmatrix} j_x & J & 1 \\ j_a & j_i & J_{12} \end{Bmatrix}(-1)^{J+j_w-j_i} \\ & \left. - \frac{Z(vi)Z_k(axwi)}{\epsilon(a)+\epsilon(x)-\epsilon(w)-\epsilon(i)}\begin{Bmatrix} j_v & J & k \\ j_a & j_w & J_{12} \end{Bmatrix}\begin{Bmatrix} j_x & J & 1 \\ j_v & j_i & k \end{Bmatrix}(-1)^{k+J_{12}+j_w+j_i-J+1}\right]. \end{aligned} \tag{A4}$$

In the above equations, the index *b* designates core states, *n* designates excited states, and *i* denotes an arbitrary core or excited state. In the sums over *i* in Eqs. (A3) and (A4), all terms with vanishing denominators are excluded. The definitions of $X_k(abcd)$ and $Z_k(abcd)$ are given by Eq. (2.12) and Eq. (2.15) in Ref. [32] and Δ_{ij} is defined at the end of Sec. II in [32]; $\epsilon(w)$ is a one-electron DF energy.

The derivative term is just the derivative of the first-order matrix element with respect to the transition energy. It is introduced to account for the first-order change in transition energy. An auxiliary quantity $P^{(\mathrm{derv})}$ is defined by

$$P^{(\mathrm{derv})}(v^0w^0[J_{12}]aJ,xJ') = \sum_{vw} \sqrt{[J_{12}][J]}P_{J_{12}}(v^0v,w^0w)\,\delta(J'x)\,\delta(vx)Z^{(\mathrm{derv})}(va)\begin{Bmatrix} j_x & J & 1 \\ j_a & j_w & J_{12} \end{Bmatrix}(-1)^{-j_a+j_w}. \tag{A5}$$

The derivative term $Z^{(\mathrm{derv})}(va)$ is given in length and velocity forms by Eqs. (10) and (11) of Ref. [31].

The coupled dipole transition matrix element between the initial state *I* and final state *F* in Na-like ions is given by

$$Q^{(1+2)}(I-F) = -\frac{1}{E^{(1)}[F]-E^{(1)}[I]}\sum_{avw}\sum_{J'_{12}} C_1^F[vw[J'_{12}]a(J)]([\epsilon(x)-\epsilon(vwa)]\{Z^{(1+2)}[vw[J'_{12}]aJ,xJ'] + B^{(2)}[vw[J'_{12}]aJ,xJ']\} + \{-E^{(1)}[F]+E^{(1)}[I]-\epsilon(x)+\epsilon(vwa)\}P^{(\mathrm{derv})}[vw[J'_{12}]aJ,xJ']). \quad \text{(A6)}$$

Here, $\epsilon(vwa)=\epsilon(v)+\epsilon(w)-\epsilon(a)$, $Z^{(1+2)}=Z^{(1)}+Z^{(\mathrm{RPA})}+Z^{(\mathrm{corr})}$. (Note that $Z^{(\mathrm{HF})}$ vanishes since we start from a Hartree-Fock basis.) The sum over vwa, J'_{12}, is understood as a sum over the complex of states with the same J and parity. In Eq. (A6), we let $B^{(2)}=B^{(\mathrm{RPA})}+B^{(\mathrm{HF})}+B^{(\mathrm{corr})}$ to represent second-order corrections arising from the Breit interaction. The quantities $C_1^F[vw[J'_{12}]a(J)]$ are eigenvectors (or mixing coefficients) for particle-particle-hole state F. The initial state I is a single, one-valence state. Using the above formulas and the results for uncoupled reduced matrix elements, we carry out the transformation from uncoupled reduced matrix elements to intermediate coupled matrix elements between physical states.

[1] M.H. Chen, Phys. Rev. A **40**, 2365 (1989).
[2] J. Nilsen, At. Data Nucl. Data Tables **41**, 131 (1989).
[3] H.L. Zhang, D.H. Sampson, R.E.H. Clark, and J.B. Mann, At. Data Nucl. Data Tables **41**, 1 (1989).
[4] R. Bruch, U.I. Safronova, A.S. Shlyaptseva, J. Nilsen, and D. Schneider, Phys. Scr. **57**, 334 (1998).
[5] R. Bruch, U.I. Safronova, A.S. Shlyaptseva, J. Nilsen, and D. Schneider, J. Quant. Spectrosc. Radiat. Transf. **60**, 605 (1998).
[6] M.A. Bautista, J. Phys. B **33**, 71 (2000).
[7] W. Eissner, M. Jones, and H. Nussbaumer, Comput. Phys. Commun. **8**, 270 (1974).
[8] J. Sugar and C. Corliss, J. Phys. Chem. Ref. Data Suppl. **2**, 100 (1985).
[9] T. Shirai, Y. Funatake, K. Mori, J. Sugar, W.L. Wiese, and Y. Nakai, J. Phys. Chem. Ref. Data **19**, 127 (1990).
[10] J.p. Buchet, M.C. Buchet-Poulizac, A. Denis, J. Desquelles, M. Druetta, S. Martin, and J.F. Wyart, J. Phys. B **20**, 1709 (1987).
[11] C. Jupén, L. Engström, R. Hutton, and E. Träbert, J. Phys. B **21**, L347 (1988).
[12] P.G. Burkhalter, L. Cohen, R.D. Cowan, and U. Feldman, J. Opt. Soc. Am. **69**, 1133 (1979).
[13] S.Y. Khakhalin, A.Y. Faenov, I.Y. Skobelev, S.A. Pikuz, J. Nilsen, and A. Osterheld, Phys. Scr. **50**, 102 (1994).
[14] V.V. Akulinichev, E.G. Kurochkina, M.E. Mavrichev, E.G. Pivinskii, V.L. Kantsyrev, and A.S. Shlyaptseva, Opt. Spectrosc. **76**, 826 (1994).
[15] V.V. Akulinichev, E.G. Pivinsky, A.S. Shlyaptseva, V.L. Kantsyrev, and I.E. Golovkin, Phys. Scr. **51**, 714 (1995).
[16] S. Bollanti *et al.*, Phys. Scr. **51**, 326 (1995).
[17] A.R. Mingaleev, S.A. Pikuz, V.M. Romanova, T.A. Shelkovenko, A.Y. Faenov, S.A. Ermatov, and J. Nilsen, Quantum Electron. **23**, 397 (1993).
[18] P. Beiersdorfer, M. Bitter, S. von Goeler, S. Cohen, K.W. Hill, J. Timberlake, R.S. Walling, M.H. Chen, P.L. Hagelstein, and J.H. Scofield, Phys. Rev. A **34**, 1297 (1986).
[19] P. Beiersdorfer, J. Nilsen, J.H. Scofield, M. Bitter, S. von Goeler, and K.W. Hill, Phys. Scr. **51**, 322 (1995).
[20] G.V. Brown, P. Beiersdorfer, H. Chen, M.H. Chen, and K.J. Reed, Astrophys. J. Lett. **557**, L75 (2001).
[21] K.J.H. Phillips, C.J. Greer, A.K. Bhatia, I.H. Coffey, R. Barnsley, and F.P. Keenan, Astron. Astrophys. **324**, 381 (1997).
[22] D. Schneider, M.H. Chen, S. Chantrenne, R. Hutton, and M.H. Prior, Phys. Rev. A **40**, 4313 (1989).
[23] P. Focke, T. Schneider, D. Schneider, G. Schiwietz, I. Kadar, N. Stolterfoht, and J.E. Hansen, Phys. Rev. A **40**, 5633 (1989).
[24] R. Hutton, D. Schneider, and M.H. Prior, Phys. Rev. A **44**, 243 (1991).
[25] D. Schneider, R. Bruch, A. Shlyaptseva, T. Brage, and D. Ridder, Phys. Rev. A **51**, 4652 (1995).
[26] S. Bliman, R. Bruch, P.L. Altick, D. Schneider, and M.H. Prior, Phys. Rev. A **53**, 4176 (1996).
[27] R. D. Cowan, *The Theory of Atomic Structure and Spectra* (University of California Press, Berkeley, CA, 1981).
[28] U.I. Safronova, W.R. Johnson, and J.R. Albritton, Phys. Rev. A **62**, 052505 (2000).
[29] U.I. Safronova, C. Namba, I. Murakami, W.R. Johnson, and M.S. Safronova, Phys. Rev. A **64**, 012507 (2001).
[30] See EPAPS Document No. E-PLRAAN-66-104211 for additional figures and tables. Figures 1–5: Transition rates for the transitions from core-excited even-parity states with $J=3/2$, 5/2 and odd-parity states with $J=1/2$–5/2 as function of Z in Na-like ions. Tables I–VIII: Possible particle-particle-hole states in the Na-like ions; jj coupling scheme; uncoupled and coupled reduced matrix elements in length and velocity forms for transitions between the odd-parity core-excited states with $J=1/2$ and the ground and singly excited states; wavelengths (in angstroms) and transition rates (A_r in 1/s) for transitions between core-excited states and excited states in Na-like ions; comparison with theoretical and experimental data. A direct link to this document may be found in the online article's HTML reference section. The document may also be reached via the EPAPS homepage (http://www.aip.org/pubservs/epaps.html) or from ftp.aip.org in the directory /epaps/. See the EPAPS homepage for more information.
[31] U.I. Safronova, W.R. Johnson, M.S. Safronova, and A. Derevianko, Phys. Scr. **59**, 286 (1999).
[32] M.S. Safronova, W.R. Johnson, and U.I. Safronova, Phys. Rev. A **53**, 4036 (1996).